Forschung im Ingenieurwesen (2023) 87:1137–1149
https://doi.org/10.1007/s10010-023-00716-0

ORIGINALARBEITEN/ORIGINALS

# Testing and modelling of a 2.5 MW wind turbine gearbox: Influence of lubricant formulation

Carlos M. C. G. Fernandes[1,2] · Rui Ferreira[1] · Jorge H. O. Seabra[2] · João M. Cruz[3] · Ricardo Bernardes[4]

Received: 10 March 2023 / Accepted: 18 September 2023 / Published online: 10 October 2023


## Abstract

This study aimed to evaluate the efficiency of different ISO VG 320 oil formulations used in a 2.5 MW wind turbine gearbox. Two commercially available lubricants, a mineral oil and a polyalphaolefin (PAO) lubricant, were tested under realistic operating conditions using a customized test rig.

Measurements showed that the overall efficiency of the mineral lubricant was higher than that of the PAO lubricant, but the difference was only 0.1% in degree of efficiency. Detailed oil analysis revealed that the mineral lubricant generated more wear particles.

A power loss model was also implemented to predict the efficiency of the gearbox, and the results of the model were found to be in agreement with the experimental results. The study concluded that the mineral oil presented higher efficiency than the PAO oil due to its lower viscosity within the narrow operating temperature range imposed on the gearbox. Nevertheless, it is important to note that the observed differences in efficiency may be attributed, in part, to measurement uncertainties and the fact that the mineral lubricant has 10% lower viscosity at the operating temperature compared to the PAO lubricant.

## Prüfung und Modellierung eines 2,5-MW-Windkraftgetriebes: Einfluss der Schmierstoffrezeptur

## Zusammenfassung

Ziel dieser Studie war es, die Effizienz verschiedener ISO VG 320-Ölformulierungen zu bewerten, die in einem 2,5-MW-Windturbinengetriebe verwendet werden. Zwei handelsübliche Schmierstoffe, ein Mineralöl und ein Polyalphaolefin (PAO)-Schmierstoff, wurden unter realistischen Betriebsbedingungen mit einem maßgeschneiderten Prüfstand getestet.

Die Messungen ergaben, dass der Gesamtwirkungsgrad des mineralischen Schmierstoffs höher war als der des PAO-Schmierstoffs, der Unterschied betrug jedoch nur 0,1 Prozentpunkte im Wirkungsgrad. Eine detaillierte Ölanalyse ergab, dass der mineralische Schmierstoff mehr Verschleißpartikel erzeugte.

Zur Vorhersage des Wirkungsgrads des Getriebes wurde außerdem ein Verlustleistungsmodell implementiert, dessen Ergebnisse mit den Versuchsergebnissen übereinstimmten. Die Studie kam zu dem Schluss, dass das Mineralöl aufgrund seiner geringeren Viskosität innerhalb des engen Betriebstemperaturbereichs des Getriebes einen höheren Wirkungsgrad aufweist als das PAO-Öl. Es ist jedoch zu beachten, dass die beobachteten Unterschiede im Wirkungsgrad zum Teil auf Messunsicherheiten und die Tatsache zurückzuführen sind, dass der mineralische Schmierstoff bei der Betriebstemperatur eine um 10% niedrigere Viskosität als der PAO-Schmierstoff aufweist.

✉ Carlos M. C. G. Fernandes
cfernandes@fe.up.pt

[1] Faculdade de Engenharia, Universidade do Porto, Rua Dr. Roberto Frias s/n, 4200-465 Porto, Portugal

[2] INEGI, Universidade do Porto Campus FEUP, Rua Dr. Roberto Frias 400, 4200-465 Porto, Portugal

[3] SERMEC-Group, 4425-348 Folgosa-Maia, Portugal

[4] VENTIENT ENERGY, Rua João Chagas, 53A Piso 0, 1495-072 Algés, Portugal

**Nomenclature**

| | |
|---|---|
| $A_c$ | carrier arrangement constant |
| $\beta$ | helix angle (°) |
| $b_p$ | planet gear face width (mm) |
| $b_s$ | sun pinion face width (mm) |
| $C_0$ | corrective factor for no-load losses |
| $c_p$ | heat capcity of the lubricant ($\mathrm{kJ\,kg^{-1}\,K^{-1}}$) |
| $CPUC$ | wear particle concentration index |
| $d$ | sample dilution factor |
| $d_{a,p}$ | planet gear tip diameter (mm) |
| $d_{a,s}$ | sun pinion tip diameter (mm) |
| $d_c$ | carrier outside diameter (mm) |
| $DL$ | large size particle index |
| $DS$ | small size particle index |
| $\eta$ | lubricant dynamic viscosity (mPa s) |
| $\eta_{\mathrm{M,G}}$ | motor or generator efficiency |
| $\eta_{\mathrm{S}}$ | system efficiency |
| $F_{\mathrm{bt}}$ | nominal transverse load in plane of action (N) |
| $f_c$ | carrier dip factor |
| $f_p$ | planet gear dip factor |
| $f_s$ | sun pinion dip factor |
| $H_{\mathrm{VL}}$ | gear loss factor |
| $ISUC$ | wear severity index |
| $\dot{m}$ | cooler oil mass flow ($\mathrm{kg\,s^{-1}}$) |
| $m_t$ | transverse module (mm) |
| $\mu_{\mathrm{bl}}$ | boundary-film coefficient of friction |
| $\mu_{\mathrm{EHL}}$ | full-film coefficient of friction |
| $\mu_{\mathrm{mZ}}$ | gear average coefficient of friction |
| $n_c$ | carrier speed (rpm) |
| $n_p$ | planet gear relative speed to carrier (rpm) |
| $N_p$ | number of planet gears |
| $n_s$ | sun pinion speed (rpm) |
| $\overline{P_{\mathrm{IN}}}$ | average input (motor) power (kW) |
| $\overline{P_{\mathrm{OUT}}}$ | average output (generator) power (kW) |
| $P$ | operating power over the rated power |
| $P_L^{\mathrm{gb}}$ | gearboxes power loss (kW) |
| $P_{\mathrm{VD}}$ | seals power loss (kW) |
| $P_{\mathrm{VL}}$ | rolling bearings power loss (kW) |
| $P_{\mathrm{VX}}$ | auxiliary power loss (kW) |
| $P_{\mathrm{VZ0}}$ | no-load gear power loss (kW) |
| $P_{\mathrm{VZ0},c}$ | planet carrier no-load losses (kW) |
| $P_{\mathrm{VZ0},p}$ | planet gear no-load losses (kW) |
| $P_{\mathrm{VZ0},s}$ | sun pinion no-load losses (kW) |
| $P_{\mathrm{VZP}}$ | load dependent gear power loss (kW) |
| $\dot{Q}_{\mathrm{cooler}}$ | cooler power (kW) |
| $R_a$ | arithmetic average roughness (µm) |
| $R_f$ | roughness factor |
| $\rho_{\mathrm{redC}}$ | curvature radius on the pitch point (mm) |
| $s_g$ | specific gravity |
| $T$ | oil temperature (°C) |
| $T_\infty$ | ambient temperature (°C) |
| $T_{\mathrm{HSSB}}$ | high speed shaft bearing temperature (°C) |
| $T_{\mathrm{in}}$ | lubricant temperature entering gearbox (°C) |
| $T_{\mathrm{ISSB}}$ | intermediate speed shaft bearing temperature (°C) |
| $T_{\mathrm{out}}$ | lubricant temperature leaving gearbox (°C) |
| $u_{\eta_{\mathrm{S}}}$ | uncertainity of the average system efficiency (%) |
| $u_{\overline{P_{\mathrm{IN}}}}$ | uncertainity of the average input power (kW) |
| $u_{\overline{P_{\mathrm{OUT}}}}$ | uncertainity of the average output power (kW) |
| $u_{\mathrm{PL}}$ | uncertainity of the average power loss (kW) |
| $v_{\sum C}$ | sum of rolling speeds on the pitch point ($\mathrm{m\,s^{-1}}$) |
| $w_c$ | carrier width (mm) |
| $X_L$ | lubricant parameter |
| gb | gearbox |
| G | generator |
| M | motor |
| S | system |

## 1 Introduction

The increasing demand for sustainable energy sources has led to a significant growth in the use of wind energy [1]. Wind turbines convert the kinetic energy present in the wind into mechanical energy, which is then converted into electrical energy. One of the key components of a wind turbine is the gearbox, which is responsible for converting the low-speed rotation of the blades into the high-speed rotation required by the electrical generator [2, 3].

The gearbox is a complex system that experiences high loads and varying operating conditions, which can lead to significant wear and fatigue failures. Lubricants play a crucial role in reducing friction, wear and surface fatigue and increasing the efficiency of the gearbox. Therefore, the selection of an appropriate lubricant formulation is essential for optimal gearbox performance [4].

Previous studies have investigated the effect of lubricant formulation on the performance of wind turbine gearboxes. A study by Liu et al. [5] evaluated the performance of a wind turbine gearbox using different lubricants, including mineral oil, synthetic ester and polyalphaolefin (PAO) lubricants. The results showed that the synthetic ester lubricant had the best performance in terms of efficiency, followed by the PAO lubricant and mineral oil. Another study by Li et al. [6] investigated the effect of lubricant viscosity on the performance of a wind turbine gearbox. The results showed that a lower viscosity lubricant led to a higher gearbox efficiency.

In addition to lubricant formulation, other factors have been found to affect the performance of wind turbine gearboxes. Temperature is one such factor, as high temperatures can lead to increased wear and tear, and reduced lubricant viscosity. A study by Zhang et al. [7] investigated the effect of temperature on the performance of a wind turbine gearbox and found that high temperatures led to increased wear and tear and reduced efficiency.

Modelling and simulation have also been used to investigate the performance of wind turbine gearboxes. Fernandes et al. implemented a power loss model for a wind turbine gearbox lubricated with different oil formulations [8]. A study by Chen et al. [9] used a dynamic model to simulate the performance of a wind turbine gearbox under different operating conditions. The results of the simulation were found to be in good agreement with experimental results and showed that the gearbox efficiency was affected by factors such as lubricant viscosity and temperature.

In conclusion, the selection of an appropriate lubricant formulation is essential for optimal gearbox performance. Previous studies have shown that the use of synthetic ester and PAO lubricants can lead to improved gearbox efficiency, while lower viscosity lubricants have also been found to improve efficiency [10–13]. Temperature has also been found to affect gearbox performance, with high temperatures leading to increased wear and tear and reduced efficiency.

Detailed experimental analyses of full-scale wind turbine gearboxes are relatively rare in the literature. However, in a previous study [14], the authors conducted experiments to measure the efficiency of a wind turbine gearbox with a power rating of 850 kW. The gearbox was lubricated with several types of oil to assess their performance.

The present study focuses on the testing and modelling of a 2.5 MW wind turbine gearbox, and the influence of lubricant formulation on the efficiency of the gearbox. Realistic operating conditions were defined using the SCADA data from a wind farm as well as the operating temperature and the wind conditions (% of the rated power) imposed to the gearbox. To further investigate the performance of the gearbox, a power loss model was implemented to predict the efficiency of the 2.5 MW gearbox.

## 2 Materials and methods

### 2.1 Gearbox

Two similar Bosch Rexroth GPV500 gearboxes were used to perform the current study. The Bosch Rexroth GPV 500 is a gearbox used in wind turbines to convert the low-speed rotation of the turbine blades into the high-speed rotation required by the electrical generator. It has three planetary stages and a final parallel helical stage as schematically shown in Fig. 1.

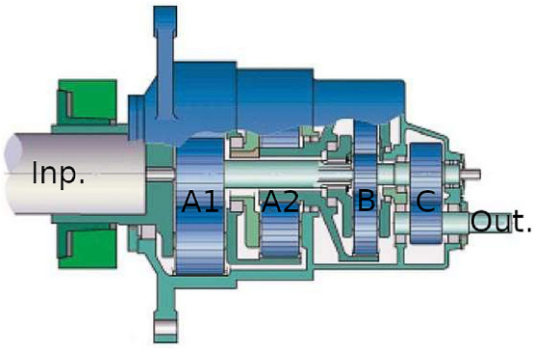


**Fig. 1** Schematic representation of the Bosch Rexroth GPV500 multiplier gearbox

The main specifications and characteristics of the gearboxes are:

- Gearbox mass: 19,500 kg;
- Gearbox arrangement:
  - power split planetary stages (A1+A2);
  - planetary stage (B);
  - helical gear stage (C).

The GPV 500 gearbox also has a lubrication system that is combined with splash lubrication to ensure that all the gear teeth and bearings are lubricated. Additionally, the GPV 500 gearbox also has a cooling system that is designed to remove heat generated during operation. The cooling system uses a combination of air and oil cooling to ensure that the gearbox is operating within the narrow recommended temperature range.

### 2.2 Test rig

The test rig used in this study is shown in Fig. 2, designed to evaluate the performance of wind turbine gearboxes under realistic operating conditions. The test rig is composed of an electrical motor (M), a generator (G), and two gearboxes (GB1 and GB2). The test gearbox GB1 is used as a speed multiplier, which means it increases the speed to match the speed required by the generator (G). The gearbox GB2 is used as a speed reducer, which means it reduces the speed of the motor to give appropriate speed conditions for the test gearbox (GB1). The electrical motor (M) is used to provide the power input to the gearboxes (nominal power plus power losses), while the generator (G) is used to impose the required nominal output power of the test gearbox (GB1).

To measure the power loss and consequently calculate the efficiency of each test, the instantaneous electric power of the motor (input power) and of the generator (output power) were recorded once per second.

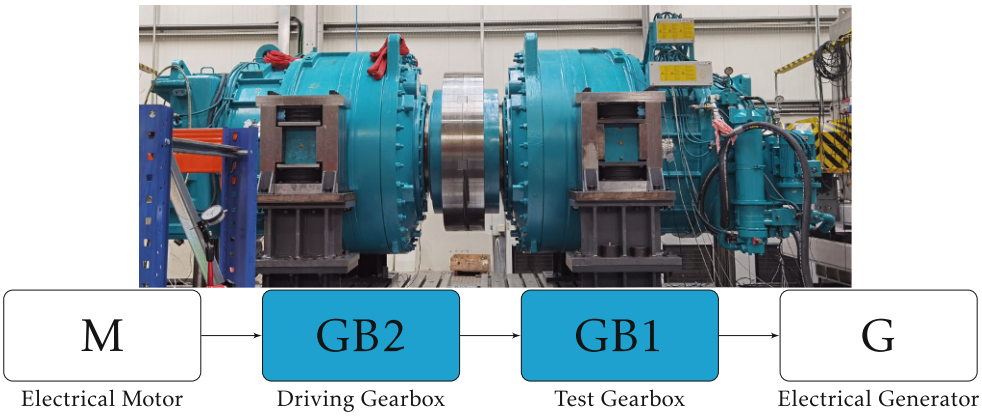


**Fig. 2** Test rig with two Bosch Rexroth GPV500 gearboxes assembled (SERMEC GROUP, Portugal)

In both gearboxes, several temperature sensors were installed at different locations to measure the temperature during the tests. These locations include the gearbox oil outlet to the cooler ($T_{out}$), gearbox oil inlet from the cooler ($T_{in}$), high speed shaft taper roller bearing with $D$ = 330.2 mm ($T_{HSSB,M}$), high speed shaft taper roller bearing with $D$ = 310 mm ($T_{HSSB,G}$), intermediate speed shaft bearing ($T_{ISSB}$) and ambient temperature ($T_{\infty}$). The ambient conditions were also measured during the tests, including the air speed in both horizontal and vertical directions, as well as the air humidity. These measurements were taken along the tests to monitor the conditions and performance of the gearbox.

## 2.3 Lubrication system

Several requirements were taken into account to ensure the proper operation of the gearboxes. One of the main considerations was the oil sump volume, which was set at 600 l according to the manufacturer specifications. Additionally, the operating manual of the gearbox from the manufacturer establishes a strict oil temperature conditions during operation and the multiplier gearbox could only operate when the oil sump temperature reached 50 °C. To lubricate the rolling bearings and gears, a mechanical oil pump was used, which is permanently in operation. The maximum oil flow of this pump is 75 l/min. These requirements were established to ensure similar conditions to field operation of the gearboxes.

The gearboxes in the system have a dedicated oil circuit that is designed to meet operating specifications. The oil circuit volume is 150 l, and the oil circuit is powered by an electric pump that circulates the oil from the oil sump to the oil cooler and back to the oil sump. The electric pump is turned on when the oil sump temperature reaches 62 °C and turned off when the oil sump temperature drops below 55 °C. The maximum oil flow of the electric pump is 105 l/min. If the oil sump temperature reaches 75 °C, a warning message is issued, and if it reaches 80 °C, the test is stopped.

A Hydac HFT 2158-BC-0035-0110-7-B-0-000 oil flowmeter was installed in each gearbox. This allowed for the measurement of the input oil flow returning from the cooler to the gearbox, which is recorded. By measuring the oil flow and the temperature gradient, it was possible to calculate the power dissipated by the oil cooling system.

## 2.4 Lubricant candidates

The lubricant candidates had the same viscosity grade, ISO VG 320, according to their product data sheets. The lubricants were formulated to achieve full EP performance, meet the requirements of the DIN-51517 part 3 (CLP) and Flender approval.

The physical properties of the oils were measured with an AND SV-10 vibro viscometer, and the results are presented in Table 1. The results showed that the kinematic viscosity at 40 °C is smaller than the value presented on the data sheet for the mineral (MIN) oil. However, the lubricant complies with the ISO VG 320 grade specified in the ISO 3448 standard.

It is evident from Fig. 3 that MIN exhibits lower viscosity within the anticipated range of operating temperatures.

## 2.5 Test procedure

The test procedure followed a set of specified operating conditions, as outlined in Table 2. These conditions are based on an analysis of SCADA data gathered during 1 year of operation, as shown in Fig. 4, using the K-means algorithm [15]. This algorithm is a method for clustering data into a specified number of clusters based on similarities in the data points. It is used to identify patterns and group similar data points together. In this case, it was likely used to analyse the SCADA data and identify specific load stages for the testing procedure.

**Table 1** Physical properties of the wind turbine gear oils.

| Parameter | Unit | MIN | PAO |
|---|---|---|---|
| Base Oil | | Mineral | poly-$\alpha$-olefin |
| Density at 15 °C | g/cm$^2$ | 0.896 | 0.867 |
| Viscosity at 40 °C | mm$^3$/s | 292.10 | 321.91 |
| Viscosity at 60 °C | mm$^3$/s | 99.49 | 127.93 |
| Viscosity at 100 °C | mm$^3$/s | 23.85 | 36.74 |
| Viscosity index | | 102 | 162 |

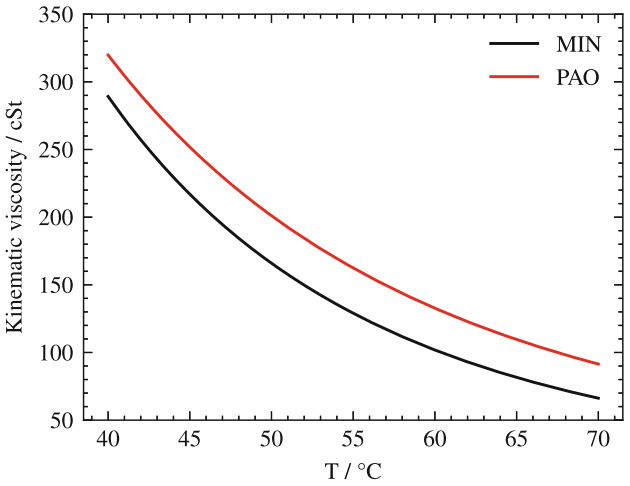


**Fig. 3** Kinematic viscosity lubricants for expected operating temperature range

**Table 2** Test conditions

| Stage | Generator Power (kW) | Motor Speed (rpm) |
|---|---|---|
| 1 | 225 | 900 |
| 2 | 725 | 1350 |
| 3 | 1285 | 1550 |
| 4 | 1870 | 1620 |
| 5 | 2500 | 1650 |

**Table 3** Ambient temperatures recorded for each test sequence

| Generator power (kW) | MIN (°C) | PAO (°C) | Δ (°C) |
|---|---|---|---|
| 225 | 18.7 | 19.8 | +1.1 |
| 725 | 19.9 | 20.0 | +0.1 |
| 1285 | 21.8 | 20.5 | –1.3 |
| 1870 | 21.9 | 20.4 | –1.5 |
| 2500 | 23.0 | 20.7 | –2.3 |

**Table 4** Ambient relative air humidity recorded for each test sequence

| Generator power (kW) | MIN (%) | PAO (%) | Δ |
|---|---|---|---|
| 225 | 51.7 | 34.6 | –17.1 |
| 725 | 50.9 | 35.7 | –15.2 |
| 1285 | 44.1 | 34.4 | –9.7 |
| 1870 | 40.7 | 33.3 | –7.4 |
| 2500 | 34.3 | 35.9 | +1.6 |

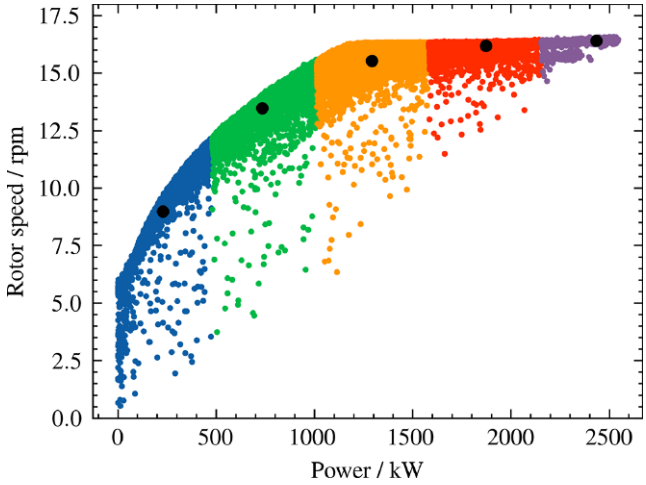


**Fig. 4** Rotor speed vs. generator power gathered from SCADA data analysis

The load stages are defined in Table 2 and they are based on the SCADA data analysis presented in Fig. 4. Each stage had a duration of 60 min.

It should be noticed that, due to the wind conditions during the period observed (1 year) the gearbox operates considerable periods at an input power which is in the range of only 9 to 51% of the rated power.

## 3 Experimental results

### 3.1 Ambient conditions

At the onset of each test stage, the ambient temperature and relative air humidity were recorded as documented in Tables 3 and 4, respectively. The recorded ambient temperatures varied between 18.7 °C and 23 °C for MIN. The largest difference in temperature within a single test sequence was 2.3 °C, which occurred for a generator power of 2500 kW, representing 10% difference.

The MIN lubricant test was exhibited to higher relative humidity values for 225 kW up to 1870 kW.

### 3.2 Oil temperature

Figure 5 illustrates the oil sump temperature leaving the gearbox to the cooler $T_{out}$ as a function of time. The data indicates that during operation at 225 kW and 725 kW, the temperature fluctuations are not consistent. It is apparent that the operation is not steady-state during these power levels.

The power dissipated in the cooler was determined using Eq. 1. The heat capacity of the lubricants was calculated using Eq. 2, where $T$ represents the oil temperature and $s_g$

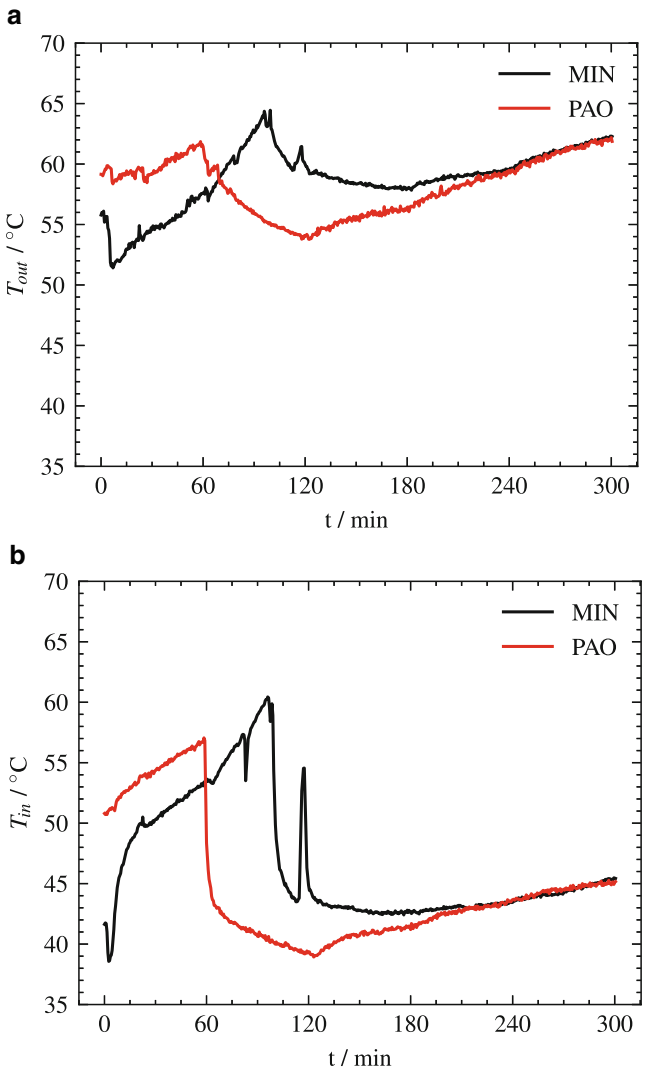


**Fig. 5** Gearbox 1 inlet and outlet temperatures. **a** Outlet temperature to the cooler, **b** Inlet temperature from the cooler

represents the specific gravity, as per the method outlined in reference [16].

$$\dot{Q}_{\text{cooler}} = \dot{m} \cdot c_p \cdot (T_{\text{out}} - T_{\text{in}}) \tag{1}$$

$$c_p = \frac{1.63 + 0.0034 \cdot T}{s_g^{0.5}} \tag{2}$$

The calculations were based on the oil density measurements obtained and reported in Table 1. Table 5 summarizes the estimated power dissipated in the cooler during the final 15 min of operation for test gearbox (GB1), with the difference being most significant during the first stage of operation.

**Table 5** Power dissipation in the cooler of test gearbox (GB1) for last 15 min

| Generator power (kW) | MIN (kW) | PAO (kW) | Δ (kW) |
|---|---|---|---|
| 225 | 13.3 | 18.9 | +5.6 |
| 725 | 46.7 | 47.8 | +1.1 |
| 1285 | 49.1 | 47.2 | –1.9 |
| 1870 | 51.2 | 50.7 | –0.5 |
| 2500 | 54.8 | 55.0 | +0.2 |

### 3.3 Rolling bearing temperatures

The temperature of the high-speed shaft rolling bearing (taper roller bearing closest to the output shaft) is presented in Table 6. From the overall analysis of the table, we can see that the temperature of the high-speed shaft rolling bearing generally increased during the five sequences.

Overall, we can see that the temperature changes between MIN and PAO were relatively small, ranging from –5.1 to +2.0 °C. However, in three stages, PAO presented higher bearing temperatures.

### 3.4 Average power loss

The instantaneous power loss in the motor, gearboxes and generator can be calculated by determining the difference between the measured input power (motor) and the output power (generator). This was done by electrically measuring the values of input and output power throughout each test stage. The measurement data was then plotted over the duration of the test campaign, as seen in Fig. 6 for the MIN candidate lubricant. This representation of the measurement data allows for the monitoring of the power loss in the gearbox and the assessment of how it changes over the course of the test campaign. It can also be used to evaluate the performance of the lubricant and the efficiency of the gearbox.

Previous research, which was conducted under laboratory conditions, has shown that steady-state conditions must be achieved in order to obtain comparable measurements of the power loss performance of different lubricants in gearboxes [10]. Therefore, in this study, the average value of the power loss was calculated during the last 15 min of

**Table 6** Average temperature of the high speed shaft bearing (taper roller bearing $D$ = 330.2 mm) for last 15 min of test gearbox

| Generator power (kW) | MIN (°C) | PAO (°C) | Δ (°C) |
|---|---|---|---|
| 225 | 60.7 | 62.7 | +2.0 |
| 725 | 68.0 | 62.9 | –5.1 |
| 1285 | 68.8 | 67.4 | –1.4 |
| 1870 | 70.6 | 70.9 | +0.3 |
| 2500 | 73.1 | 73.7 | +0.6 |

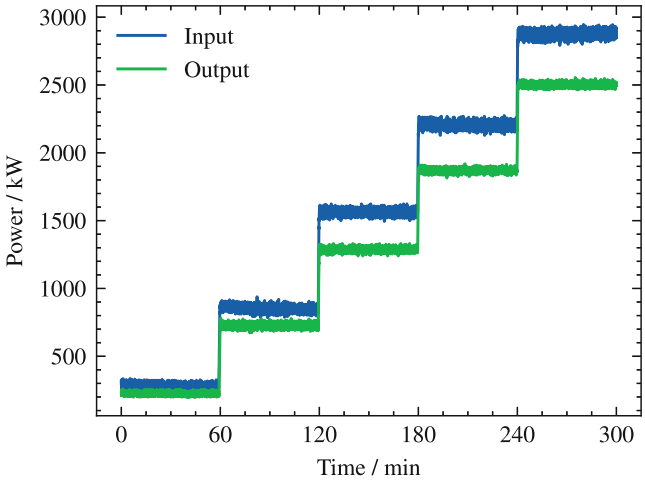


**Fig. 6** Motor input power and generator output power measured, for MIN lubricant

each load stage, and is presented in Table 7. This approach ensures that the measurements obtained during the test campaign are representative of the steady-state conditions and can be used to accurately evaluate the performance of the test gearbox.

Table 7 shows the average power loss for the last 15 min of operation for different generator power levels. The table shows also the average power loss values for both lubricants as well as the difference Δ = PAO – MIN between the two values. Figure 7 shows the average power loss values for the Mineral and PAO oils, as well as other reference PAO's previously tested on the same gearboxes and test rig taken here as reference.

The results indicate that the MIN lubricant performs better than the PAO lubricant, as the power loss values are lower for the MIN lubricant in all cases. The difference in power loss between the two lubricants ranges from 1.10 to 11.68 kW, with the highest difference observed at the power level of 725 kW. The smallest difference is observed at the lowest power level of 225 kW, with a difference of only 1.10 kW.

Overall, the results suggest that using the MIN lubricant promotes a power loss reduction of 0.06% (2500 kW) to 1.6% (725 kW) and consequently improve the efficiency of the wind turbine gearbox.

**Table 7** Average power loss for last 15 min

| Generator power (kW) | MIN (kW) | PAO (kW) | Δ (kW) |
|---|---|---|---|
| 225 | 60.9 | 62.0 | +1.1 |
| 725 | 120.3 | 132.0 | +11.7 |
| 1285 | 276.5 | 281.2 | +4.7 |
| 1870 | 332.8 | 338.1 | +5.3 |
| 2500 | 380.2 | 381.7 | +1.5 |

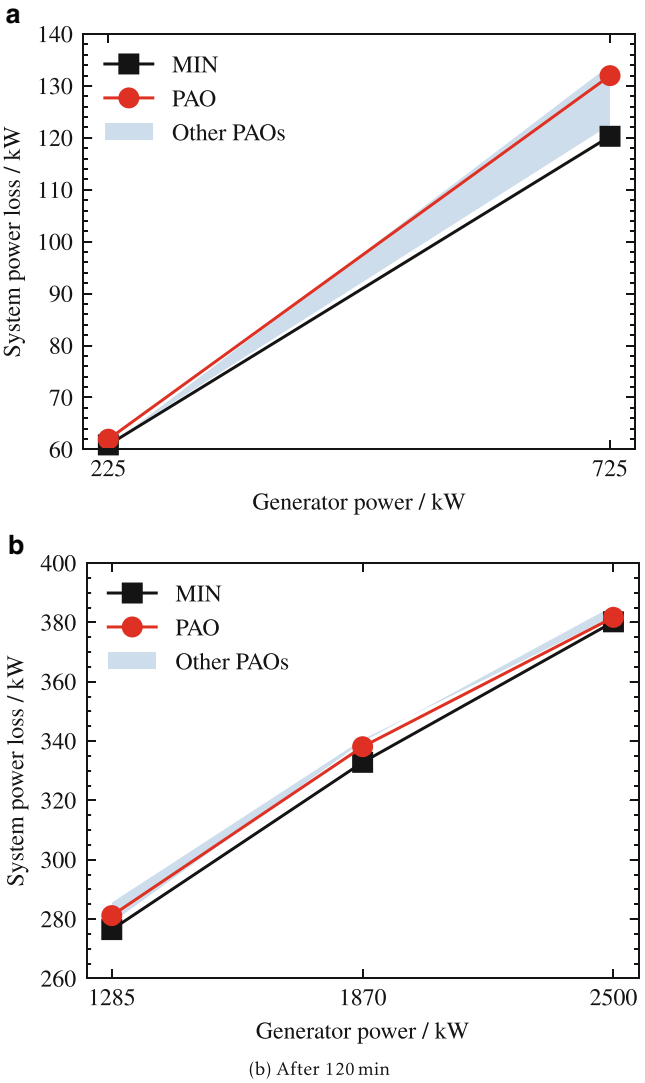


**Fig. 7** Average system (motor, gearboxes and generator) power loss for each lubricant candidate during the last 15 min. **a** Up to 120 min, **b** after 120 min

## 3.5 Average efficiency

The test rig imposes the generator power ($P_{OUT}$) and the input power ($P_{IN}$) of the driving gearbox connected to the electrical motor is influenced by the overall efficiency of the system. The overall efficiency was calculated according to the following Eq. 3:

$$\eta_S = \frac{\overline{P_{OUT}}}{\overline{P_{IN}}} \tag{3}$$

Where $\overline{P_{OUT}}$ and $\overline{P_{IN}}$ are the average values of the output and input power, respectively. The values calculated are given in Table 8.

The results indicate that the efficiency of the system is slightly lower when using the PAO lubricant compared to

**Table 8** Average efficiency during the last 15 min

| Generator power (kW) | MIN (%) | PAO (%) | Δ |
|---|---|---|---|
| 225 | 78.77 | 78.48 | –0.43 |
| 725 | 85.79 | 84.62 | –0.14 |
| 1285 | 82.30 | 82.05 | –0.36 |
| 1870 | 84.89 | 84.69 | –0.10 |
| 2500 | 86.80 | 86.76 | –0.12 |

the MIN lubricant, as the efficiency values for PAO are lower than those for MIN in all cases. The difference in efficiency between the two lubricants ranges from –0.43% to –0.10%, with the largest difference observed at the lowest power level of 225 kW. The smallest difference is observed at the highest power level of 2500 kW.

Overall, the results suggest that using the PAO lubricant may not improve the efficiency of the wind turbine generator as observed in previous studies using different gearbox architectures [12–14]. However, the differences are small, and the choice of lubricant should be based on other factors such as wear protection, cost, and environmental impact. Further studies are needed to investigate these factors and provide a more comprehensive analysis of the performance of different lubricants in wind turbine gearboxes.

### 3.6 Uncertainty of power loss and efficiency measurements

In this study, the estimation of power loss and efficiency in the system relied on measurements of motor input power and generator output power. To account for measurement variability, the standard deviation was calculated for both sets of measurements. The propagation of uncertainties using subtraction rules was applied to determine the uncertainty associated with the average power loss, as given by Eq. 4. Similarly, Eq. 5 was used to calculate the uncertainty for the average efficiency. In both cases, a 95% confidence level was considered with a corresponding z-value of 1.96.

$$u_{\mathrm{PL}} = \sqrt{u^2_{\overline{P_{\mathrm{IN}}}} + u^2_{\overline{P_{\mathrm{OUT}}}}} \tag{4}$$

$$u_{\eta_{\mathrm{S}}} = \eta_{\mathrm{S}} \cdot \sqrt{\left(\frac{u_{\overline{P_{\mathrm{IN}}}}}{\overline{P_{\mathrm{IN}}}}\right)^2 + \left(\frac{u_{\overline{P_{\mathrm{OUT}}}}}{\overline{P_{\mathrm{OUT}}}}\right)^2} \tag{5}$$

The results of the uncertainty analysis are presented in Table 9 for both lubricants. The calculated uncertainties for efficiency fall within the observed differences between the lubricants. Therefore, based on the available data, it can be concluded that there is no significant difference between the candidate lubricants. So, it is recommended to conduct further repetitions of each test to confirm these findings.

**Table 9** Uncertainty of average power loss and average efficiency measurements during the last 15 min

| Generator power (kW) | $u_{\mathrm{PL}}$ | | $u_{\eta_{\mathrm{S}}}$ | |
|---|---|---|---|---|
| | MIN (kW) | PAO (kW) | MIN (%) | PAO (%) |
| 225 | 1.25 | 1.28 | 0.39 | 0.39 |
| 725 | 1.61 | 1.62 | 0.17 | 0.17 |
| 1285 | 1.59 | 1.63 | 0.09 | 0.09 |
| 1870 | 1.66 | 1.62 | 0.07 | 0.07 |
| 2500 | 1.71 | 1.74 | 0.05 | 0.05 |

## 4 Power loss modelling

To create a model that can accurately predict the efficiency of a gearbox, it is necessary to consider the various sources of power loss. These sources include those related to the gears, rolling bearings, and seals, as well as any additional losses that may exist from auxiliary devices connected to the mechanism as shown in Fig. 8.

### 4.1 Model equations and coefficients

The calculation of no-load gear power losses was performed in accordance with the ISO/TR 14179-2 standard [17]. To determine the load-independent gear losses, Mauz's model was employed. This model is included in ISO TR 14179-2 [17] and provides a method for estimating the total hydraulic torque loss in a splash lubricated parallel axis gear stage.

The hydraulic torque loss, denoted as $T_H$, is computed using the following equation:

$$T_H = C_{\mathrm{Sp}} \cdot C_1 \cdot e^{C_2 \cdot \left(\frac{v_t}{v_{t0}}\right)} \tag{6}$$

Hydraulic length can be obtained from equation (7):

$$l_h = \frac{4 \cdot A_{\mathrm{Gearbox}}}{U} \tag{7}$$

where $A_{\mathrm{Gearbox}}$ is area of the gearbox cross section and $U$ is the perimeter of the gearbox cross section.

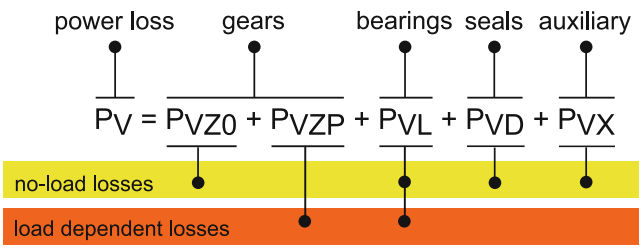


**Fig. 8** Power loss sources [11]

The splash oil factor, $C_{\mathrm{Sp}}$, depends on the immersion depth and the factors $C_1$ and $C_2$ are used to account for the effect of tooth width and immersion depth. These factors are given by Eqs. 8, 9 and 10, respectively.

Since no viscosity effect was measurable in low depths and for high immersion depth the effects were contradictory, this formulation does not account such effect.

$$C_{\mathrm{Sp}} = \left(\frac{4h_{e,\max}}{3h_c}\right)^{1,5} \cdot \frac{2h_c}{l_h} \tag{8}$$

$$C_1 = 0.063 \cdot \left(\frac{h_{e1} + h_{e2}}{h_{e0}}\right) + 0.0128 \cdot \left(\frac{b}{b_0}\right)^3 \tag{9}$$

$$C_2 = \frac{h_{e1} + h_{e2}}{80 \cdot h_{e0}} + 0.2 \tag{10}$$

where the reference values for immersion depth, gear width and tangential speed are defined as follows: $h_{e0} = 10\,\mathrm{mm}$, $b_0 = 10\,\mathrm{mm}$ and $v_{t0} = 10\,\mathrm{m/s}$.

On any gearbox, gear load-independent power loss will be the sum of each stage no-load gear loss. This type of loss can be calculated by multiplying the no-load torque loss by the angular velocity.

$$P_{\mathrm{VZ0},h} = T_H \cdot \frac{\pi \cdot n_i}{30} \tag{11}$$

with $n$ as the number of stages.

The calculation of gear power losses for the planetary stages was performed based on the ISO/TR 14179-1 standard [17], which is also presented in ANSI/AGMA 6123-C16 [18]. For the sun pinion, the following equation is applicable:

$$P_{\mathrm{VZ0},s} = \frac{A_c \cdot f_s \cdot \nu \cdot n_s^3 \cdot d_{a,s}^{4.7} \cdot b_s \cdot \left(\frac{R_f}{\sqrt{\tan\beta}}\right)}{10^{26}} \tag{12}$$

where $R_f = 7.93 - \frac{4.648}{m_t}$ and $m_t$ is the transverse module.

For the planet gears:

$$P_{\mathrm{VZ0},p} = \frac{A_c \cdot f_p \cdot \nu \cdot n_p^3 \cdot d_{a,p}^{4.7} \cdot b_p \cdot \left(\frac{R_f}{\sqrt{\tan\beta}}\right)}{10^{26}} \cdot N_p \tag{13}$$

For the case of the planet carrier, Eq. 14 was used.

$$P_{\mathrm{VZ0},c} = \frac{A_c \cdot f_c \cdot \nu \cdot n_c^3 \cdot d_c^{4.7} \cdot w_c}{10^{26}} \tag{14}$$

The factors $f_s$, $f_p$ and $f_c$ are based on the degree of immersion of the element in the oil. Since windage effects for typical industrial gear reducers are negligible with respect to the other losses, the dip factor is 0 when the element does not dip in the oil. When the element is fully submerged in the oil, the factor is 1. When the element is partially submerged in the oil, linearly interpolate between 0 and 1 [18].

The total churning power loss of a planetary stage is given by Eq. 15. A corrective factor $C_0$ was added which allowed to fit the model prediction with the experiments measurements. For the present case a factor $C_0 = 3.77$ was found for all tested conditions and lubricants.

$$P_{\mathrm{VZ0}} = \left(P_{\mathrm{VZ0},s} + P_{\mathrm{VZ0},p} + P_{\mathrm{VZ0},c} + P_{\mathrm{VZ0},h}\right) \cdot C_0 \tag{15}$$

Ohlendorf (1958) [19] presented an approach for calculating the power loss that occurs during gear tooth contact, as stated in Eq. 16, which is a function of the input power ($P_{\mathrm{IN}}$), gear loss factor ($H_{\mathrm{VL}}$) [20, 21], and coefficient of friction ($\mu_{\mathrm{mZ}}$) [22, 23].

$$P_{\mathrm{VZP}} = P_{\mathrm{IN}} \cdot H_{\mathrm{VL}} \cdot \mu_{\mathrm{mZ}} \tag{16}$$

The coefficient of friction is typically assumed to be constant along the path of contact and can be estimated based on Schlenk's equation 17 [22] or Fernandes et al. [23] equation.

$$\mu_{\mathrm{mZ}} = 0.048 \cdot \left(\frac{F_{\mathrm{bt}}/b}{\upsilon_{\sum C} \cdot \rho_{\mathrm{redC}}}\right)^{0.2} \cdot \eta^{-0.05} \cdot R_a^{0.25} \cdot X_L \tag{17}$$

The lubricant factor for the present analysis was derived based on FZG gear tests [10, 11] and the values are resumed in Table 10. The values from ISO TR 14179 are given as reference.

The lubricants shown in Table 10, correspond to ISO VG 320 wind turbine gearbox oils according to [11] (a mineral (MIN) and a poly-alpha-olefin (PAO).

According to SKF [24], the total torque loss in rolling bearings is the sum of the rolling frictional moment, sliding frictional moment, seal moment and drag moment.

Based on the findings of Fernandes et al. [11], it can be argued that the values for $\mu_{\mathrm{bl}}$ and $\mu_{\mathrm{EHL}}$, presented in Table 11, provide more accurate power loss predictions for wind turbine gear oils.

The values presented in Table 11, derived based on rolling bearing tests [11], are to be used on bearings that

**Table 10** Oil parameter for different formulations

| Oil | $X_L$ (Fernandes) [11] | $X_L$ (ISO TR 14179) [17] |
|---|---|---|
| MIN | 0.846 | 1 |
| PAO | 0.666 | 0.8 |

**Table 11** Values for $\mu_{EHL}$ and $\mu_{bl}$ proposed by Fernandes et al. [10]

| Oil | | TBB | RTB |
|---|---|---|---|
| MIN | $\mu_{bl}$ | 0.058 | 0.035 |
| | $\mu_{EHL}$ | 0.056 | 0.018 |
| PAO | $\mu_{bl}$ | 0.049 | 0.039 |
| | $\mu_{EHL}$ | 0.044 | 0.010 |

are not tapered roller bearings. The thrust ball bearings (TBB) values can be used in calculations related to elliptic contact bearings, similarly the roller thrust bearings (RTB) values can be used for line contact bearings.

The seals power loss were predicted using by Freudenberg equation [25].

### 4.2 Gearboxes power loss

An examination of the test apparatus used revealed that the measured power loss encompasses contributions from both the motor (M) and generator (G). By utilizing the efficiency curves provided by the manufacturers of the motor and generator, a polynomial equation, as represented in Eq. 18 was defined.

$$\eta_{M,G} = -16.78P^4 + 60.89P^3 - 84.76P^2 + 53.49P + 84.95 \quad (18)$$

where $P$ is the ratio of the operating power over the rated power 2600 kW of the motor/generator.

Based on the predicted efficiency curve of the motor (M) and generator (G), the following calculation was made to estimate the experimental power loss of the gearboxes (GB1+GB2):

$$P_L^{gb} = \overline{P_{IN}} \times \eta_M \left( \frac{\overline{P_{IN}}}{2600} \right) - \frac{\overline{P_{OUT}}}{\eta_G \left( \frac{\overline{P_{OUT}}}{2600} \right)} \quad (19)$$

Given the observed similarities in behaviour among the motor and generator across all tests, it is believed that the majority of the discrepancy in power loss can be attributed to variations in lubricant performance within the gearboxes.

### 4.3 Model validation

The accuracy of the power loss model was evaluated by comparing it to the results calculated with Eq. 19. Direct comparison was challenged by two limitations. Firstly, the motor/generator manufacturer provided the efficiency curve only for a nominal power greater than 650 kW. Secondly, experiments conducted at 225 kW and 725 kW exhibited a transient temperature behaviour common to the beginning of testing and due to the usage of resistance heaters to maintain an operating temperature of at least 50 °C, as required by the gearbox manufacturer (as shown in Fig. 5). The precise power provided by the heaters was not recorded due to limitations in the acquired test rig system. These limitations and uncertainties led to significant deviations between the measurements and the power loss model values. Therefore, model validation will only be conducted using testing conditions that occurred after 120 min or at higher operating power where no heaters are needed to keep the lubricant temperature above 50 °C.

The validation of the model and the partitioning of power loss sources (churning, gears, bearings, and seals), for the MIN reference, is depicted in Fig. 9a. The coefficient of determination between the model and the experiments was $R^2 = 0.970$. The maximum relative error for the last three load stages between the model and the experiments was 6.1% for 1285 kW. The last two stages showed an error around 1%. This indicates that the model is capable of accurately predicting power loss for steady-state operation and it can be used as a reliable tool for assessing power loss in real-world applications. Figure 9b depicts a comparison between the power loss model and experimental results for the PAO lubricant. The coefficient of determination between the model and experiments is $R^2 = 0.953$. The highest relative error for the last three load stages between the model and experiments is 6% for 1285 kW and 2% for 1870 kW. Moreover, the relative error at the rated power of 2500 kW is 0.5%.

### 4.4 Influence of viscosity on the power loss sources

It is important to note that the optimal viscosity for a particular application depends on various factors, including the gearbox design, operating temperature, and load characteristics. In some cases, an excessively high viscosity may cause problems such as churning, which can increase the power losses. Therefore, the selection of the appropriate lubricant viscosity or the optimal operating temperature range for each lubricant must consider all of these factors to achieve the best performance and minimize power losses. The current section allow to observe the effect of kinematic viscosity on the different power loss sources.

The primary factors influencing the predicted power loss include gearbox size, oil volume, and tangential velocity of the gears. As these factors remained constant for all tested lubricants, viscosity and density were the distinguishing factors among the candidates. Figure 10 illustrates the predicted power loss as a function of the kinematic viscosity, calculated based on the oil output temperature of each gearbox. The results indicate that higher kinematic viscosity results in higher power loss.

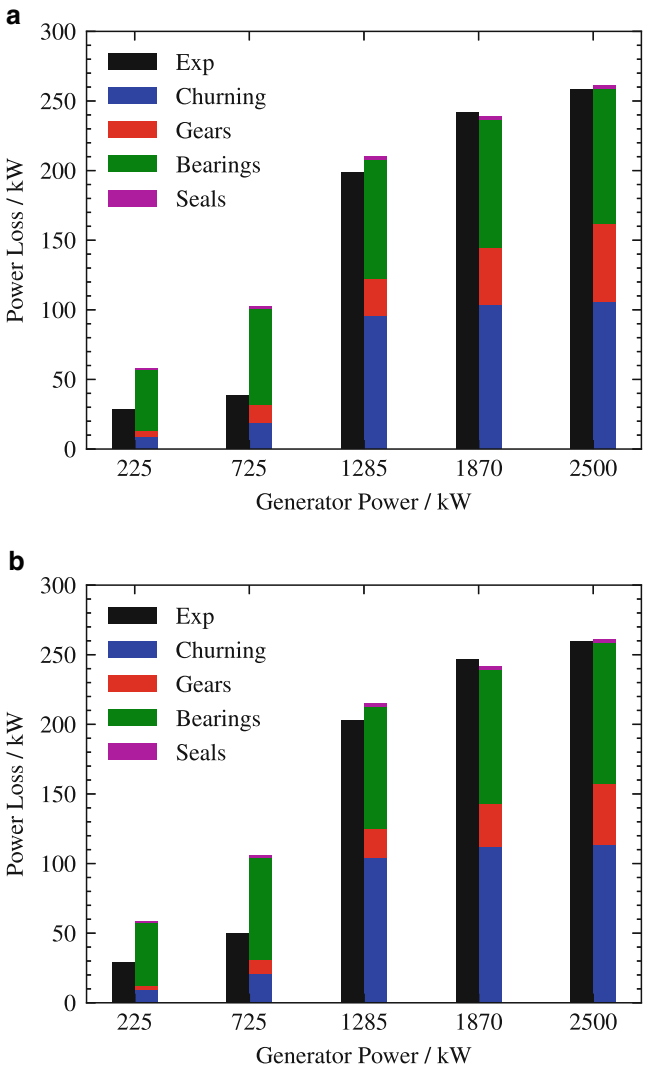


**Fig. 9** Model verification and power loss partition (GB1+GB2). **a** MIN ($R^2$ = 0.970), **b** PAO ($R^2$ = 0.953)

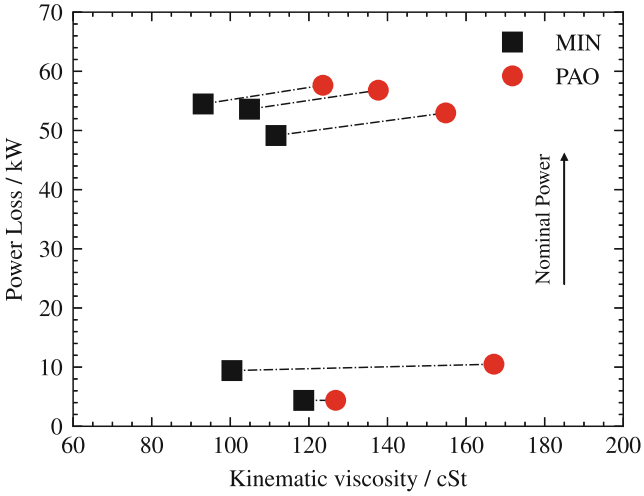


**Fig. 10** Predicted load independent gear power losses versus operating kinematic viscosity for test gearbox (GB1)

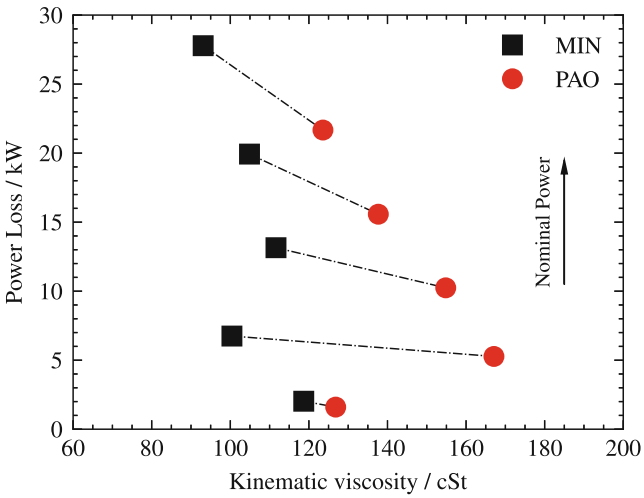


**Fig. 11** Predicted load dependent gears power loss versus operating kinematic viscosity for test gearbox (GB1)

The load-dependent gear power losses are presented in Fig. 11 as a function of the operating kinematic viscosity. As shown in the figure, a higher viscosity results in a reduction of the coefficient of friction and, consequently, the load-dependent gear losses. In addition to the lubricant viscosity, the lubricant's chemical composition and additives also affect gear power losses. For instance, as previously mentioned, synthetic lubricants are expected to exhibit lower gear power losses compared to mineral-based lubricants due to their superior chemical properties and additive packages. In the implemented model, this is taken into account through lubricant factor $X_L$. Therefore, careful selection of the lubricant type and formulation can result in significant power loss savings and improved gearbox efficiency [10, 12].

As shown in Fig. 12, the MIN reference lubricant produced lower power loss on the bearings, primarily due to the rolling and drag loss, which are largely influenced by the lubricant's viscosity. The driving gearbox, operating at the highest temperature and with a higher load, exhibited even lower power loss, indicating that the viscosity of the lubricants is the key factor.

## 5 Oil analysis

In this study, three techniques were used to analyse oil samples collected from the gearboxes after the test campaign: ferrography, direct reading ferrometry, and particle counting. The results of these techniques were used to draw conclusions about the wear and degradation of the oil samples.

The results of ferrometry revealed that the MIN oil sample generated greater wear indexes as shown in Table 12.

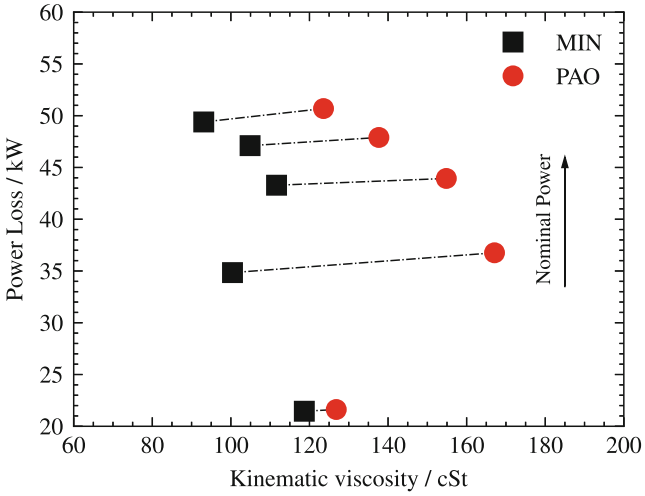


**Fig. 12** Predicted rolling bearings power loss versus operating kinematic viscosity for test gearbox (GB1)

**Table 12** Wear indexes (ferrometry) and cleanliness codes (particle counting)

| | MIN | PAO |
|---|---|---|
| *d* | 1 | 1 |
| *DL* | 10.4 | 2.6 |
| *DS* | 5.9 | 2.6 |
| *CPUC* | 16.3 | 5.2 |
| *ISUC* | 73.4 | 0.0 |
| ISO 4406:17 | 21/17/12 | 16/15/13 |

The results of analytic ferrography showed a significant presence of polar particles in the MIN oil sample taken from test gearbox (GB1), which are typical of the degradation of additive compounds under high shear stress. There was agreement between the particle count results and the ferrography results shown in Fig. 13.

## 6 Conclusion

The overall efficiency measured with the mineral lubricant for all tested conditions was found to be higher than that measured using the PAO lubricant. However, the difference in the overall efficiency at 2.5 MW operating power was only 0.1% . The experimental tests were complimented with detailed oil analysis to verify the wear particle generation for each lubricant candidate and in this regard, mineral lubricant presented the highest amount of wear particles.

The friction generated between the meshing teeth, churning losses, shaft seals and rolling bearing losses were included in the model. The agreement between the power loss model and the experiments was achieved. The power loss model allowed to verify that both gears churning and rolling bearings are the major sources of energy loss.

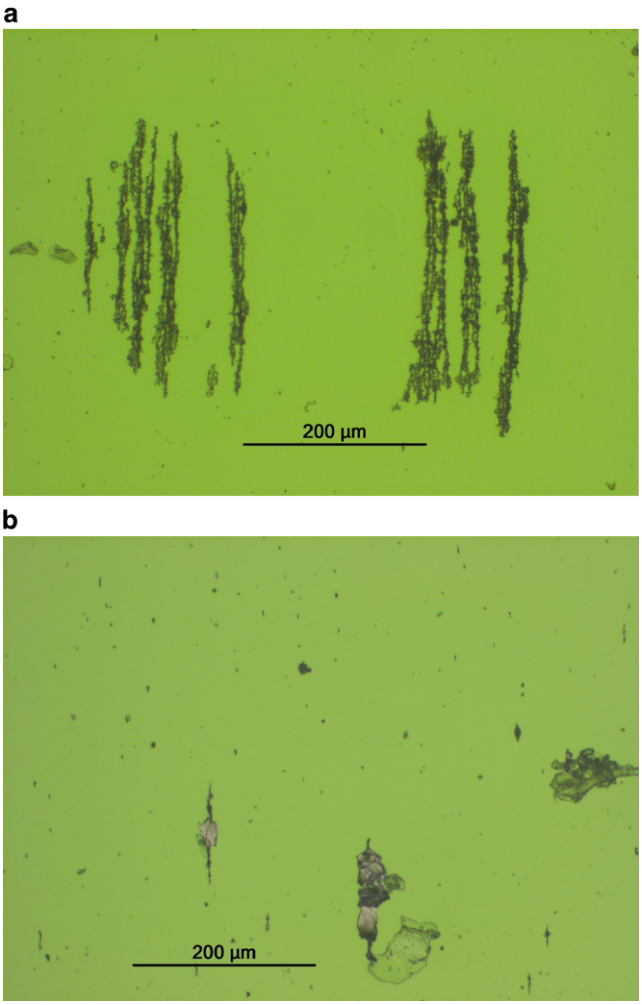


**Fig. 13** Ferrography analysis of oil candidates after testing taken from test gearbox (GB1). **a** MIN sample, **b** PAO sample

Based on both the experimental results and the model analysis, it can be concluded that the mineral oil demonstrated higher efficiency compared to the PAO oil under the specific operating conditions employed. This can be attributed to the lower viscosity of the mineral oil within the prescribed narrow temperature range for the gearbox. However, due to the inherent viscosity differences and the presence of additional measurement uncertainties, the precise influence of oil formulation could not be reliably quantified in the present study.

The results of this study have important implications for the design and operation of wind turbines, as they demonstrate the importance of selecting the appropriate lubricant formulation and operating temperature range for optimal gearbox performance. This paper provides a comprehensive analysis of the effect of lubricant formulation on the efficiency of a 2.5 MW wind turbine gearbox, and offers insights for future research in this field.

**Funding** The authors gratefully acknowledge the funding whom without this work would not have been possible: LAETA under the project UID/50022/2020.

**Funding** Open access funding provided by FCT|FCCN (b-on).



## References

1. - (2001) High efficiency planetary gearboxes for eco-power. World Pumps 2001(419):34–36. https://doi.org/10.1016/S0262-1762(01)80327-8
2. Ozgener O, Ozgener L (2007) Exergy and reliability analysis of wind turbine systems: A case study. Renew Sustain Energy Rev 11(8):1811–1826. https://doi.org/10.1016/j.rser.2006.03.004
3. Hur S, Leithead W (2016) Collective control strategy for a cluster of stall-regulated offshore wind turbines. Renew Energy 85:1260–1270. https://doi.org/10.1016/j.renene.2015.07.087
4. Sarker BR, Faiz TI (2016) Minimizing maintenance cost for offshore wind turbines following multi-level opportunistic preventive strategy. Renew Energy 85:104–113. https://doi.org/10.1016/j.renene.2015.06.030
5. Liu P, Feng W, Liu P, Chen X (2018) Effect of lubricant formulations on wind turbine gearbox performance. Renew Energy 118:658–664
6. Li Q, Li J, Sun H, Zhao Z (2019) The effect of lubricant viscosity on the performance of wind turbine gearbox. J Renew Sustain Energy 11(5):53301
7. Zhang X, Wang Q, Sun Y (2020) Effect of temperature on the performance of a wind turbine gearbox. J Renew Sustain Energy 12(2):23303
8. Fernandes CM, Hammami M, Martins RC, Seabra JH (2016) Power loss prediction: Application to a 2.5 MW wind turbine gearbox. Proc Inst Mech Eng Part J: J Eng Tribol 230(8):983–995. https://doi.org/10.1177/1350650115622362
9. Chen J, Li H, Chen Z, Zhang J, Chen X (2021) Investigation of the wind turbine gearbox performance using dynamic modeling and simulation. Energy Convers Manag 246:114150
10. Fernandes CM, Martins RC, Seabra JH (2014) Torque loss of type C40 FZG gears lubricated with wind turbine gear oils. Tribol Int 70(0):83–93. https://doi.org/10.1016/j.triboint.2013.10.003
11. Fernandes CM, Marques PM, Martins RC, Seabra JH (2015) Gearbox power loss. Part I: Losses in rolling bearings. Tribol Int 88(0):298–308. https://doi.org/10.1016/j.triboint.2014.11.017
12. Fernandes CM, Marques PM, Martins RC, Seabra JH (2015) Gearbox power loss. Part II: Friction losses in gears. Tribol Int 88:309–316. https://doi.org/10.1016/j.triboint.2014.12.004
13. Fernandes CM, Marques PM, Martins RC, Seabra JH (2015) Gearbox power loss. Part III: Application to a parallel axis and a planetary gearbox. Tribol Int 88:317–326. https://doi.org/10.1016/j.triboint.2015.03.029
14. Fernandes CM, Blazquez L, Sanesteban J, Martins RCRC, Seabra JH (2016) Energy efficiency tests in a full scale wind turbine gearbox. Tribol Int 101:375–382. https://doi.org/10.1016/j.triboint.2016.05.001
15. Pedregosa F, Varoquaux G, Gramfort A, Michel V, Thirion B, Grisel O, Blondel M, Prettenhofer P, Weiss R, Dubourg V, Vanderplas J, Passos A, Cournapeau D, Brucher M, Perrot M, Duchesnay E (2011) Scikit-learn: Machine learning in Python. J Mach Learn Res 12:2825–2830
16. Stachowiak GW, Batchelor AW (2014) ENGINEERING TRIBOLOGY, 4th edition. Elsevier
17. - (2001) ISO TR 14179-2, Gears - Thermal capacity - Part 2: Thermal load-carrying capacity
18. - (2021) ANSI/AGMA 6123-C16, Design Manual for Enclosed Epicyclic Gear Drives, Standard, American Gear Manufacturers Association, 1001 N. Fairfax Street, Suite 500, Alexandria, Virginia 22314
19. Ohlendorf H (1958) Verlustleistung und Erwärmung von Stirnradverzahnungen. Ph.D. thesis. Technische Universität München
20. Fernandes CMCG, Marques PMT, Martins RC, Seabra JHO (2015) Influence of gear loss factor on the power loss prediction. Mech Sci 6(2):81–88. https://doi.org/10.5194/ms-6-81-2015
21. Wimmer AJ (2006) Lastverluste von Stirnradverzahnungen, Konstruktive Einflüsse, Wirkungsgradmaximierung, Tribologie. Fakultät für Maschinenwesen der Technischen Universität München
22. Höhn B-RR, Michaelis K, Völlmer T (1996) Thermal Rating of Gear Drives Balance Between Power Loss and Heat Dissipation. AGMA Tech Pap 96:12
23. - (2016) Coefficient of friction equation for gears based on a modified Hersey parameter. Tribol Int 101:204–217. https://doi.org/10.1016/j.triboint.2016.03.028
24. SKF (2017) The SKF model for calculating the frictional moment. SKF
25. Simrit (1976) Radialwellendichtringe (Katalog Nr. 100)